Metal-Insulator Transition and Its Relation to Magnetic Structure in $(LaMnO_3)_{2n}/(SrMnO_3)_n$ Superlattices

A. Bhattacharya,[1,2,*] S. J. May,[1] S. G. E. te Velthuis,[1] M. Warusawithana,[3] X. Zhai,[3] Bin Jiang,[4] J.-M. Zuo,[4] M. R. Fitzsimmons,[5] S. D. Bader,[1,2] and J. N. Eckstein[3]

[1]*Materials Science Division and Argonne National Laboratory, Argonne, Illinois 60439, USA*
[2]*Center for Nanoscale Materials, Argonne National Laboratory, Argonne, Illinois 60439, USA*
[3]*Department of Physics and University of Illinois at Urbana-Champaign, Urbana-Champaign, Illinois 60801, USA*
[4]*Department of Materials Science and Engineering, University of Illinois at Urbana-Champaign, Urbana-Champaign, Illinois 60801, USA*
[5]*Los Alamos National Laboratory, Los Alamos, New Mexico 87545, USA*

(Received 25 February 2007; published 27 June 2008)

Superlattices of $(LaMnO_3)_{2n}/(SrMnO_3)_n$ ($1 \leq n \leq 5$), composed of the gapped insulators $LaMnO_3$ and $SrMnO_3$, undergo a metal-insulator transition as a function of n, being metallic for $n \leq 2$ and insulating for $n \geq 3$. Measurements of transport, magnetization, and polarized neutron reflectivity reveal that the ferromagnetism is relatively uniform in the metallic state, and is strongly modulated in the insulating state, being high in $LaMnO_3$ and suppressed in $SrMnO_3$. The modulation is consistent with a Mott transition driven by the proximity between the $(LaMnO_3)/(SrMnO_3)$ interfaces. The insulating state for $n \geq 3$ obeys variable range hopping at low temperatures. We suggest that this is due to states at the Fermi level that emerge at the $(LaMnO_3)/(SrMnO_3)$ interfaces and are localized by disorder.

DOI: 10.1103/PhysRevLett.100.257203 PACS numbers: 75.47.Lx, 71.30.+h, 73.20.Fz, 73.21.Cd

An interface between two strongly correlated materials creates a distinct environment for allowing new collective states to emerge. In bulk samples of the strongly correlated manganite $La_{1-x}Sr_xMnO_3$, the A site is populated randomly by La^{3+} and Sr^{2+} cations, allowing the Mn cation on the B site to have a mixed valence of Mn^{3+}/Mn^{4+}, which leads to electron itinerancy and double-exchange mediated ferromagnetism for a range of x [1]. The end members of the phase diagram are both antiferromagnetic (AFM) insulators. $LaMnO_3$ (LMO) with nominally Mn^{3+} $t_{2g}^3 e_g^1$ occupancy is an insulator with strong Mott-Hubbard or charge-transfer Coulomb correlations in a half-filled e_g band [2] and forms an A-type orbital-ordered AFM [ferromagnetic (FM) in-plane, AFM between planes] at low temperatures. At the other end, $SrMnO_3$ (SMO) with Mn^{4+} with $t_{2g}^3 e_g^0$ occupancy is a band insulator with G-type or cubic AFM order. With current state-of-the-art techniques [3], atomically sharp SMO/LMO interfaces can be created where charge leakage may lead to mixed-valence states at coherent two-dimensional (2D) layers. The correlations between the spin, charge, and orbital degrees of freedom at the interface may give rise to states that are distinct from LMO, SMO, or any part of the randomly alloyed phase diagram. At an ideal LMO/SMO interface, the electron hopping amplitude t between e_g states on neighboring Mn^{3+}/Mn^{4+} sites depends on the alignment between the Mn spins via double exchange. A nonzero t causes the electronic profile at the interface to be intrinsically smeared, i.e., electrons "leak" from the Mn^{3+} sites on LMO into the Mn^{4+} sites in SMO. This competes with the attractive Coulomb potential, which binds the electron to the LMO in order to maintain charge neutrality. The length scale for charge leakage [4] is given by $L_{\mathrm{TF}} = a(\frac{t}{e^2/\varepsilon a})$, where ε is the dielectric function and a is the lattice constant, and is estimated to be 1–3 unit cells (u.c.), depending upon the values of ε and t. In analogy with the titanates [5], this interface could also have a finite density of states (DOS) at the Fermi energy (E_F) [6], which may be spin polarized due to interfacial ferromagnetism.

It is known that in short-period superlattices [e.g., $(LMO)_{2n}/(SMO)_n$ for $n = 1$] where the LMO/SMO interfaces are brought into close proximity, the transport and magnetic properties are quite similar to those of the corresponding random alloy [7], while at large periods ($n > 3$), an insulator is obtained. It is useful to think about this in terms of a Mott transition [8], in which the attractive Coulomb potential is screened by electrons from the neighboring SMO/LMO interface. Below a critical separation, the screening weakens the binding potential to the extent that electrons become delocalized between the interfaces. This gives rise to a homogeneous 3D charge distribution similar to the random alloy, but without the A-site disorder [9,10]. Upon increasing the separation between interfaces, the screening weakens and electrons become bound near the La^{3+} ions, and strong modulation of electron density and the concomitant order parameters is expected within the superlattice. In order to realize such a system, the interfaces need to be chemically abrupt on a length scale shorter than L_{TF}, such that the leakage effects can be separated from those of chemical intermixing. A direct measurement of the underlying structure of the relevant order parameters at these buried interfaces would then allow us to study the consequences of charge leakage [11] and relate this to the emergent properties of the superlattices.

In this Letter, we investigate highly ordered digital superlattices of $(LaMnO_3)_{2n}/(SrMnO_3)_n$ with well-defined interfaces where the intermixing is limited to within about 2 Å. For $n \leq 2$, a FM metal is obtained, with relatively uniform ferromagnetism, closely related in properties to those of the corresponding random alloy $La_{0.67}Sr_{0.33}MnO_3$. For $n \geq 3$, the superlattices are insulating at the lowest T. Using neutron reflectivity, we show that for $n \geq 3$ the ferromagnetism is also strongly modulated with a periodicity commensurate with the superlattice, with suppression of ferromagnetism in the $SrMnO_3$. Furthermore, the localized states that emerge for $n \geq 3$ are not like the gapped states observed in LMO or SMO, but rather are states near E_F that have been localized by disorder. We suggest that these localized states are interfacial in nature, and that the disorder that localizes them may have an intrinsic magnetic origin due to frustrated spins between adjacent AFM and FM layers within these structures.

Superlattices of $[(LMO)_{2n}/(SMO)_n]_p$, where n, p are integers and $3np \sim 80$, were grown on strontium titanate (001) substrates etched in dil-HCl, with ozone-assisted molecular beam epitaxy [9]. Grazing and high angle x-ray scattering confirm that the structures have smooth interfaces (~2 Å interfacial roughness) over macroscopic distances [Fig. 1(a)]. Scanning transmission electron microscopy (STEM) of an $n = 4$ sample revealed atomically sharp interfaces between the $SrMnO_3$ and $LaMnO_3$ layers, with unit-cell high steps [Fig. 1(b)] [12]. The $n = 1$ superlattice peak is best fit by an interfacial LMO/SMO interfacial roughness of 2.3 Å (less than one unit cell). When this roughness is increased to 4 Å in simulations, the peak disappears into the noise of the measurement.

The in-plane resistivity (ρ) vs temperature (T) is shown in Fig. 2 for a series of digital superlattices from $n = 1$ up to $n = 5$, and compared to a random-alloy film of identical composition $La_{0.67}Sr_{0.33}MnO_3$. The $\rho(T)$ increases by over 8 orders of magnitude with increasing n at the lowest T. Near the nominal Curie temperature T_C, all superlattices show a drop in ρ (for $n = 5$, T_C is ~40 K less than the temperature for the downturn in ρ). The $n = 1$ superlattice has a lower ρ at low T than the random alloy, probably a result of lower impurity scattering of charge carriers. At any given T, ρ increases upon increasing n, and an insulator is obtained at the lowest T for $n \geq 3$. A 20 u.c. film of LMO grown on strontium titanate (STO) under identical conditions was insulating and obeyed $\rho = \rho_0 \exp(E_A/kT)$ with $E_A = 125$ meV above the magnetic ordering temperature of 150 K, where there is an inflection. This film was found to be FM with a saturation moment $M_S = 3.25\mu_B$/Mn (averaged over SMO and LMO layers). The FM behavior in these very thin films [13] may be due to strain and/or a deficiency of La. Superlattices of $(SMO)_3/(LMO)_1$ (corresponding to $x = 0.75$) were also found to be strongly insulating (Fig. 2, inset), and no signatures of magnetic ordering could be detected with a SQUID (superconducting quantum interference device) magnetometer. The T_C value for the random-alloy $La_{0.67}Sr_{0.33}MnO_3$ film is 355 K and the saturation magnetization $M_S = 3.22\mu_B$/Mn, while for the $n = 1$ superlattice, $T_C = 340$ K and $M_S = 3.0\mu_B$/Mn. The coercivity H_c is nearly identical between the two samples at 10 K. For the $n = 1$ sample, if we assume a maximum possible FM moment of $4\mu_B$/Mn in the LMO layers, we can set a lower bound on the FM moment in the SMO layers of $1\mu_B$/Mn, in order for M_S to be equal to the measured value. The great similarity in resistivity and magnetic properties between the random alloy and the $n = 1$ sample, however, points to a more homogeneous electronic and magnetic structure within the $n = 1$ sample.

As n increases, the value of H_c increases, and that of M_S is strongly suppressed for $n \geq 3$ [Fig. 3]. In order to probe the underlying magnetic order that gives rise to this behavior, we have used polarized neutron reflectometry (PNR) to measure the magnetic structure for wave vectors perpendicular to the plane ($q_\perp$) in a $(LMO)_{11.8}(SMO)_{4.4}$

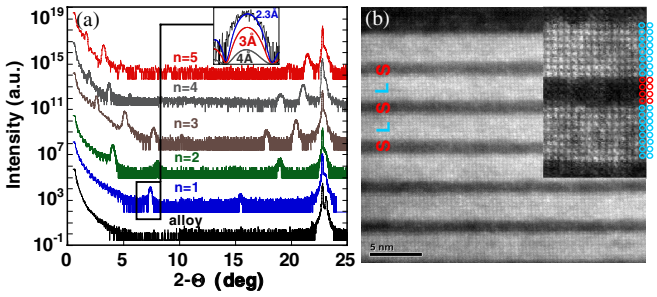

FIG. 1 (color online). (a) X-ray reflectivity and diffraction for $n = 1$ to 5. Simulations of the first superlattice peak for $n = 1$ (inset) are shown for roughnesses of 2.3 Å, 3 Å, and 4 Å. (b) STEM z-contrast images from an $n = 4$ superlattice showing $(LMO)_8/(SMO)_4$ regions, labeled L and S. Rows of atoms are shown on the right as a guide to the eye.

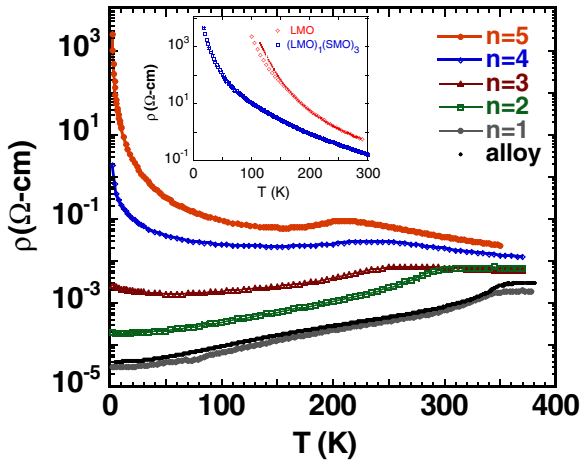

FIG. 2 (color online). Resistivity of $La_{0.67}Sr_{0.33}MnO_3$ random-alloy film, and corresponding $(SrMnO_3)_n/(LaMnO_3)_{2n}$ superlattices, $1 \leq n \leq 5$. The inset shows the resistivity of a pure $LaMnO_3$ thin film with a fit of $\rho = \rho_0 \exp(E_A/kT)$ with $E_A = 125$ meV to the data, and also the resistivity of a $(SrMnO_3)_3/(LaMnO_3)_1$ superlattice for reference.

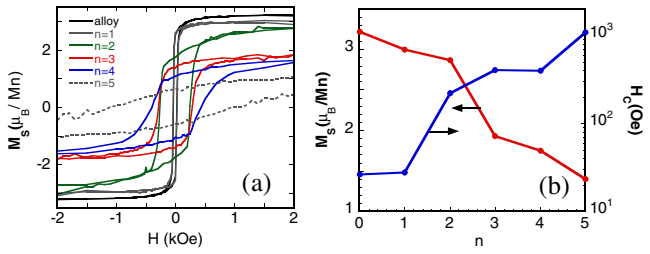

FIG. 3 (color online). (a) Average magnetization vs H for $n = 1$ to 5 at $T = 10$ K. (b) Evolution of the saturation magnetization and coercivity at 10 K with increasing n.

(similar in transport and magnetic behavior to $n = 5$, henceforth called $n = 5'$) and an $n = 3$ superlattice. PNR measurements were carried out at ASTERIX [14] at the Los Alamos Neutron Scattering Center of Los Alamos National Laboratory. Figure 4(a) shows the PNR data at 300 K (well above T_C) in a field of 5.5 kOe. The reflectivity for the two neutron spin states R^+ and R^- (parallel and opposite to the applied magnetic field, respectively) is the same. Because of the similarity in the nuclear scattering length for La and Sr, the structural Bragg peak at $q_\perp = 0.108$ Å^{-1} is barely visible. After field cooling in 5.5 kOe to 10 K [Fig. 4(b)], there is a significant difference between R^+ and R^-, a strong Bragg peak emerges at $q_\perp = 0.103$ Å^{-1}, and a second order peak is visible near $q_\perp = 0.2$ Å^{-1}. According to our best fit to the PNR data [15], the magnetization is strongly modulated commensurate with the superlattice period, with a maximum near $3.8\mu_B$/Mn within the $LaMnO_3$, and a minimum of less than $0.1\mu_B$/Mn in the $SrMnO_3$. This rules out all scenarios that would allow a reduced moment with a uniform distribution (e.g., a uniformly canted AFM state) amongst the various layers. The integrated magnetization in the superlattice extracted from PNR is found to be within 6% of the M_S ($\sim 1.9\mu_B$/Mn at 5.5 kOe) measured with a SQUID magnetometer. For $n = 3$ at $T = 10$ K, we also observe a magnetic Bragg peak at $q \sim 0.175$ Å^{-1}, corresponding to a modulated magnetization. The calculated reflectivities that best reproduce the data suggest an amplitude for the modulation that is lower in magnitude than in the $n = 5$ sample.

Since $L_{TF} \sim 1$–3 u.c., we would expect that for $n > 3$ the LMO/SMO interfaces are relatively isolated from one another, and the in-plane transport properties of the superlattices are related to those for a single interface. We note that $\rho(T < 30$ K) for the $n = 4$ superlattice is more than 10^4 lower than the LMO film at 100 K, and 10^2 lower than the $(SMO)_3/(LMO)_1$ superlattice. The ρ is also 10^3 lower than known values for SMO films [7] on STO at 400 K. Thus, the high n superlattices are *not* like either SMO or LMO. We find that for $n \geq 3$, ρ for $T = 2$–28 K is consistent with Mott's variable range hopping in 3D, i.e., $\rho = \rho_0 \exp(T_0/T)^{1/4}$ [Fig. 5(a)]. In this scenario, there is a nonzero DOS at E_F. Recent resonant x-ray scattering experiments at the O-K edge in an $n = 4$ superlattice observed the signatures of a DOS that emerges at the LMO/SMO interface with the onset of FM order [11]. However, these states are localized due to disorder, and their exponential tails decay over a characteristic localization length ξ_L. The charge carriers move between local sites via thermally assisted hops, preferentially to sites close in energy, over distances $L_{\text{hop}} \sim \xi_L(T_0/T)^{1/4}$. From the values of T_0 obtained from fitting to the data, the localization length can be calculated from the expression $\xi_L = \{[18/k_B T_0 N(E_F)]\}^{1/3}$, where $N(E_F)$ is the DOS at E_F [16]. For the $n = 3$ sample that lies near the border of the metal-insulator transition, $\xi_L = 180$ Å. For the $n = 4$

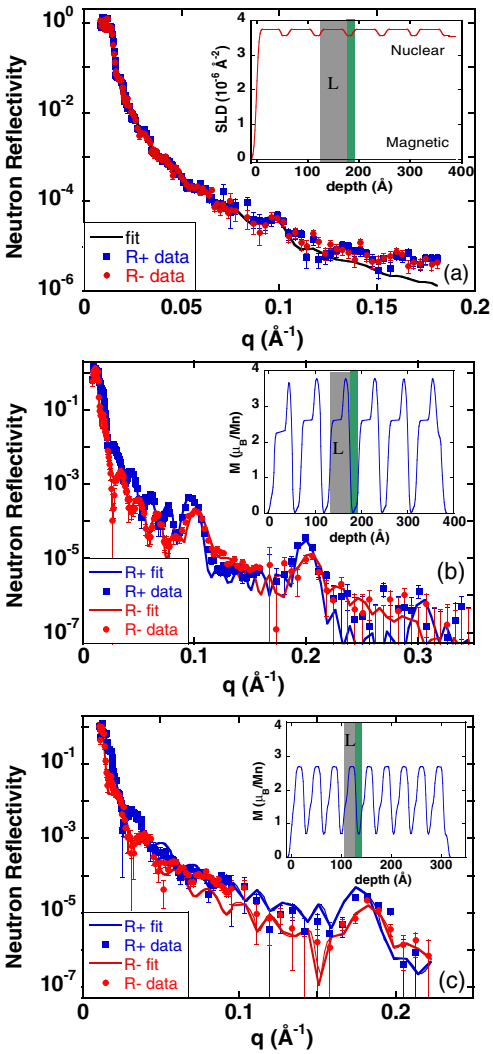

FIG. 4 (color online). (a) Polarized neutron reflectivity measurements of an $n = 5$ superlattice at 300 K and (inset) the nuclear scattering potential of the superlattice, with zero magnetization. The gray region is the extent of LMO in one superlattice period, and the green is the SMO. (b) PNR at 10 K in a field of 5.5 kOe ($T_C = 180$ K). The inset shows the inferred magnetic structure from the best fit. (c) PNR measurements for the $n = 3$ sample, and (inset) the inferred magnetic structure from a calculation that best reproduced the data.

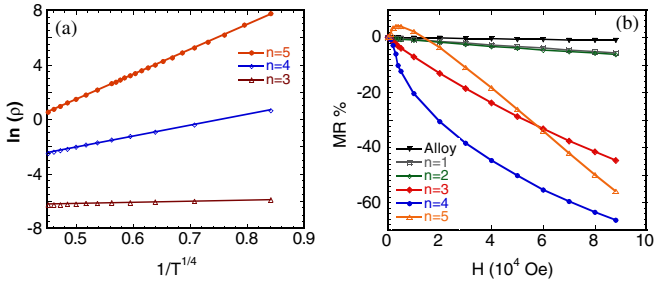

FIG. 5 (color online). (a) Fit of the low temperature data for the $n = 3$–5 superlattices to the form for Mott's variable range hopping in 3D: $\rho = \rho_0 \exp(T_0/T)^{1/4}$. (b) MR at 10 K. The insulating superlattices ($n \geq 3$) show a higher value of magnetoresistance (>44.5% at 88 kOe) than the metallic samples ($n \leq 2$) (<6.3% at 88 kOe). The $n = 5$ superlattice shows a positive MR at low fields, with a maximum value at 4 kOe.

superlattice, $\xi_L = 11.4$ Å, and $L_{\text{hop}}(10\text{ K}) = \sim 18.5$ Å at 10 K, while for the $n = 5$, $\xi_L = 3.6$ Å, and $L_{\text{hop}} \sim 14$ Å at 10 K. For $n = 4$ and 5, the ξ_L is smaller than the distance between the two nearest LMO/SMO interfaces. The hopping exponent is consistent with 3D transport. This suggests that the carriers are localized in regions of extent ξ_L near a single interface but can hop between states near different interfaces. We note that the estimates for L_{TF} used here assume that ε is a constant. However, in the vicinity of a metal-insulator transition, ε diverges as the metallic state is approached, and can be related to ξ_L for a disorder driven transition [17]. The variation in ε with n needs to be accounted for in realistic estimates of L_{TF}.

The PNR data indicate that the high n superlattices have FM regions next to non-FM regions. If the non-FM regions are AFM, then we expect to observe the consequences of competing AFM/FM interactions with magnetic pinning, frustration, and canted order. We have measured the magnetoresistance (MR), defined as $[R(H) - R(0)]/R(0)$, where H is the magnetic field. The insulating superlattices have MR that is 7 times or greater in magnitude than the metallic superlattices at 10 K and 88 kOe [Fig. 5(b)], with no indication of saturation. This is indicative of canted/frustrated due to competing AFM/FM interactions [18], that are better aligned by an external magnetic field. Furthermore, for the $n = 5$ sample, the MR is *positive* at low fields and changes sign at higher fields. Positive MR has also been observed in multilayers with complex magnetic structure, with coexisting FM and AFM couplings [19]. At this time we do not have a clear mechanism, though the symmetric nature of the signal in magnetic field and lack of hysteresis points to an origin that is neither grain boundaries nor spin-polarized tunneling [20]. Further evidence for the proximity of AFM/FM regions is the emergence of magnetic pinning with increasing n as evidenced by an increase in H_c from 20 Oe for the $n = 1$ superlattice to 1100 Oe for a $n = 5$ sample [Fig. 3].

In conclusion, we have established that the metal-insulator transition in $(\text{LMO})_{2n}/(\text{SMO})_n$ superlattices is accompanied by a strongly modulated FM order in the insulating state. The insulator that emerges for $n \geq 3$ is consistent with a finite DOS at E_F, with states localized by disorder. A metal is obtained when these interfaces are brought into close proximity, consistent with a Mott transition. The intimate coexistence of phases with different order parameters within the high-n superlattices may give rise to a large susceptibility to external electric and magnetic fields, and holds the promise of engineering new types of mixed-phase and interfacial materials.

This work was supported by the U.S. Department of Energy, Office of Basic Energy Sciences under Contracts No. DE-AC02-06CH11357 (at Argonne), No. DEFG02-91-ER45439, No. DE-FG02-07ER46453, and No. DE-FG02-07ER46471 (at the UIUC Frederick Seitz Materials Research Lab), and No. DE-AC52-06NA25396 (at Los Alamos National Lab's Lujan Neutron Scattering Center at LANSCE.)

*anand@anl.gov

[1] Y. Tokura and Y. Tomioka, J. Magn. Magn. Mater. **200**, 1 (1999).
[2] I. Loa *et al.*, Phys. Rev. Lett. **87**, 125501 (2001); A. Yamasaki *et al.*, *ibid.* **96**, 166401 (2006).
[3] J. Verbeeck *et al.*, Phys. Rev. B **66**, 184426 (2002).
[4] C. Lin, S. Okamoto, and A. J. Millis, Phys. Rev. B **73**, 041104(R) (2006).
[5] S. Okamoto and A. Millis, Phys. Rev. B **70**, 241104 (2004); S. S. Kancharla and E. Dagotto, *ibid.* **74**, 195427 (2006).
[6] A. Ohtomo *et al.*, Nature (London) **419**, 378 (2002); S. Okamoto and A. J. Millis, *ibid.* **428**, 630 (2004).
[7] T. Koida *et al.*, Phys. Rev. B **66**, 144418 (2002); P. A. Salvador *et al.*, Appl. Phys. Lett. **75**, 2638 (1999); C. Adamo *et al.*, Appl. Phys. Lett. **92**, 112508 (2008).
[8] N. F. Mott, Philos. Mag. **6**, 287 (1961).
[9] A. Bhattacharya *et al.*, Appl. Phys. Lett. **90**, 222503 (2007).
[10] D. Akahoshi *et al.*, Phys. Rev. Lett. **90**, 177203 (2003).
[11] S. Smadici *et al.*, Phys. Rev. Lett. **99**, 196404 (2007).
[12] Images were acquired on a JEOL 2010F transmission electron microscope operating in STEM mode with an annular dark field detector.
[13] C. Aruta *et al.*, J. Appl. Phys. **100**, 023910 (2006).
[14] M. R. Fitzsimmons and C. F. Majkrzak, *Modern Techniques for Characterizing Magnetic Materials*, edited by Y. Zhu (Kluwer, Boston, 2005).
[15] S. May *et al.*, Phys. Rev. B **77**, 174409 (2008).
[16] N. F. Mott, *Metal-Insulator Transitions* (Taylor & Francis, London, 1990), 2nd ed.; M. Viret, L. Ranno, and J. M. D. Coey, Phys. Rev. B **55**, 8067 (1997).
[17] Y. Imry, Y. Gefen, and D. J. Bergman, Phys. Rev. B **26**, 3436 (1982).
[18] C. Leighton *et al.*, Phys. Rev. Lett. **84**, 3466 (2000).
[19] I. N. Krivorotov *et al.*, Phys. Rev. Lett. **86**, 5779 (2001).
[20] See EPAPS Document No. E-PRLTAO-101-080852 for a supplementary figure. For more information on EPAPS, see http://www.aip.org/pubservs/epaps.html.